Osteoarthritis and Cartilage 22 (2014) 111–120

Osteoarthritis and Cartilage

High molecular weight hyaluronic acid regulates osteoclast formation by inhibiting receptor activator of NF-κB ligand through Rho kinase

W. Ariyoshi †, T. Okinaga †, C.B. Knudson ‡, W. Knudson ‡, T. Nishihara †*

† Division of Infections and Molecular Biology, Department of Health Promotion, Kyushu Dental University, Kitakyushu, Fukuoka, Japan
‡ Department of Anatomy and Cell Biology, The Brody School of Medicine, East Carolina University, Greenville, NC, USA

ARTICLE INFO

Article history:
Received 13 June 2013
Accepted 22 October 2013

Keywords:
Hyaluronic acid
Osteoclast
Receptor activator of NF-κB ligand
CD44
RhoA

SUMMARY

Objective: To determine the effects of high molecular weight hyaluronic acid (HMW-HA) on osteoclast differentiation by monocytes co-cultured with stromal cells.
Methods: Mouse bone marrow stromal cell line ST2 cells were incubated with HMW-HA or 4-methylunbeliferone (4-MU) for various times. In some experiments, cells were pre-treated with the anti-CD44 monoclonal antibody (CD44 mAb) or Rho kinase pathway inhibitors (simvastatin or Y27632), then treated with HMW-HA. The expression of receptor activator of NF-κB ligand (RANKL) was determined using real-time reverse transcription polymerase chain reaction (RT-PCR), western blotting, and immunofluorescence microscopy, while the amount of active RhoA was measured by a pull-down assay. To further clarify the role of HMW-HA in osteoclastogenesis, mouse monocyte RAW 264.7 cells were co-cultured with ST2 cells pre-stimulated with $1,25(OH)_2D_3$. Osteoclast-like cells were detected by staining with tartrate-resistant acid phosphatase (TRAP).
Results: HMW-HA decreased RANKL mRNA and protein expressions, whereas inhibition of hyaluronic acid (HA) synthesis by 4-MU enhanced RANKL expression. Blockage of HA-CD44 binding by CD44 mAb suppressed HMW-HA-mediated inhibition of RANKL. Pull-down assay findings also revealed that HMW-HA transiently activated RhoA in ST2 cells and pre-treatment with CD44 mAb inhibited the activation of RhoA protein mediated by HMW-HA. Moreover pre-treatment with Rho kinase pathway inhibitors also blocked the inhibition of RANKL by HMW-HA. Co-culture system results showed that HMW-HA down-regulated differentiation into osteoclast-like cells by RAW 264.7 cells induced by $1,25(OH)_2D_3$-stimulated ST2 cells.
Conclusions: These results indicated that HA-CD44 interactions down-regulate RANKL expression and osteoclastogenesis via activation of the Rho kinase pathway.

Introduction

Hyaluronan, or hyaluronic acid (HA), is an unsulfated long polysaccharide chain comprised of repeating disaccharide units of *N*-acetylglucosamine and glucuronic acid, and a major component of the extracellular matrix (ECM). HA is present with a high molecular mass in mammalian bone marrow and connective tissues, as well as skin, vitreous humor of the eye, cartilage, and umbilical cord tissue. Unlike other glycosaminoglycans, it is synthesized as a free polysaccharide, rather than substituted on a core protein, and newly synthesized HA polymers of 2,500–25,000 repeating disaccharides have a molecular mass ranging from 10^3–10^4 kDa. The roles of HA range from purely structural functions to regulation of several cellular responses including proliferation, differentiation, motility, adhesion and gene expression.[1,2]

High molecular weight hyaluronic acid (HMW-HA) is clinically used as a symptom- or disease-modifying drug for non-surgical treatments of joints as well as cartilage diseases such as osteoarthritis (OA)[3], as the efficacy of articular HA therapy for OA has been demonstrated in animal experimental models[4,5] and clinical trials[6,7]. Although the underlying mechanisms may be due to its chondroprotective and anti-inflammatory effects, the precise roles of HA in the pathogenesis of OA remain largely unknown.

Many connective tissue cells exhibit a large HA and proteoglycan-rich pericellular matrix that is tethered to the cell surface via interactions with the HA receptor CD44[8], a

* Address correspondence and reprint requests to: T. Nishihara, 2-6-1 Manazuru, Kokurakita-ku, Kitakyushu 803-8580, Japan. Tel: 81-93-285-3050; Fax: 81-93-581-4984.
E-mail addresses: arikichi@kyu-dent.ac.jp (W. Ariyoshi), t-oki@kyu-dent.ac.jp (T. Okinaga), knudsonc@ecu.edu (C.B. Knudson), knudsonw@ecu.edu (W. Knudson), tatsujin@kyu-dent.ac.jp (T. Nishihara).

1063-4584/$ – see front matter
http://dx.doi.org/10.1016/j.joca.2013.10.013

multifunctional transmembrane glycoprotein that exhibits extensive molecular heterogeneity. The CD44 ectodomain is responsible for the binding of HA, while the cytoplasmic domain regulates specific signaling such as RhoA-activated Rho kinase[9], Rho/Rac1-specific guanine nucleotide exchange factors (p115RhoGEF[10], Tiam1[11], and Vav2[12]), c-Src kinase[13], and transforming growth factor-β receptors[14]. CD44 also directly binds to cytoskeletal proteins such as ankyrin and ERM (ezrin, radixin, moesin).[15]

Bone remodeling is a highly regulated process involving the coordinated action of osteoblasts and osteoclasts. Osteoclasts originate from hematopoietic precursors of a monocyte/macrophage lineage and differentiate into multinucleated giant cells specialized to resorb bone by fusion of mononuclear progenitors[16]. It has also been shown that osteoclast precursors must interact with osteoblasts/stromal cells to differentiate into mature osteoclasts[17], while osteoclast formation is induced in the presence of the receptor activator of the NF-κB ligand (RANKL), a member of the tumor necrosis factor (TNF) superfamily, which is expressed by osteoblasts/bone stromal cells. RANKL interacts with the osteoclast cell surface receptor RANK, which in turn recruits TNF receptor-associated factors (TRAFs)[18], and plays a crucial role in the osteoclast differentiation axis.

It is possible that receptor-mediated effects of HA and derivatives lead to changes in the metabolism of chondrocytes[19,20], synoviocytes[21,22], and subchondral bone osteoblasts[23], and several researchers have reported the involvement of HA in osteoclast formation and resorption[24,25]. In a previous study, we demonstrated that low molecular weight HA (LMW-HA, molecular weight <8 kDa) enhanced both osteoclast formation and function *in vitro*[26]. However, scant attention has been given to the effects of HMW-HA on osteoclast-supporting cells. In the present study, we examined the effects of HMW-HA on osteoclastogenesis and found that it suppressed osteoclast formation via down-regulation of RANKL in bone marrow derived osteoblastic/stromal cells *in vitro*.

Methods

Reagents and antibodies

High molecular weight HA (HMW-HA, molecular weight 2,500 kDa) was supplied by Seikagaku Corp. (Tokyo, Japan), while 4-methylumberlliferone (4-MU) was purchased from Sigma–Aldrich (St. Louis, MO, USA). The anti-RANKL polyclonal antibody was obtained from R&D Systems Inc. (Minneapolis, MN, USA), anti-β-actin monoclonal antibody from Sigma–Aldrich and anti-RhoA monoclonal antibody from Cell Signaling Technology Inc. (Beverly, MA, USA).

Cell cultures

Mouse bone marrow stromal cells ST2 was obtained from Riken Cell Bank (Ibaraki, Japan) and maintained in alpha-minimum essential medium (α-MEM; GIBCO, Grand Island, NY, USA) supplemented with 10% fetal calf serum (FCS; Sigma–Aldrich), 100 U/ml penicillin G (Meiji Seika Pharm Co., Tokyo, Japan), and 100 μg/ml streptomycin (Wako Pure Chemical Industries, Osaka, Japan) at 37°C in an atmosphere of 5% CO_2. ST2 cells were incubated with HMW-HA or 4-MU for various times. For some experiments, cells were pre-treated with the anti-CD44 monoclonal antibody (10 μg/ml, Calbiochem, San Diego, CA, USA), simvastatin (10 μM, Sigma–Aldrich), or Y27632 (10 μM, Calbiochem), then treated with HMW-HA (50 μg/ml) in the continuing presence or absence of each reagent.

Detection of cell surface HA and RANKL

ST2 cells were treated in 8-well chamber slides (5×10^3 cells/well), then fixed with 4% paraformaldehyde in phosphate buffered saline (PBS, pH 7.4) for 1 h, quenched with 0.2 M glycine in PBS, and blocked with 1% bovine serum albumin (BSA, Sigma–Aldrich) in PBS for 1 h. For HA detection, the cells were incubated with 2.0 μg/ml of a biotinylated-HA binding protein (HABP) probe (Seikagaku Corp.) overnight at 4°C. Following extensive washing, the cells were incubated with 1 μg/ml neutravidin-fluorescein isothiocyanate (FITC) (1:1,000) (Invitrogen, Carlsbad, CA, USA) in PBS containing 1% BSA for 1 h at 4°C.

For immunofluorescence analysis of RANKL, fixed cells were incubated overnight with the anti-RANKL antibody (1:100), then for 1 h at room temperature with FITC conjugated anti-goat IgG (Santa Cruz Biotechnology, Santa Cruz, CA, USA). To visualize stress fibers, cells were incubated with rhodamine phalloidin (Invitrogen) for 20 min at room temperature, then washed, mounted in mounting medium containing the nuclear stain, 4′6-diamidino-2-phenylindole dihydrochloride (DAPI; Vector Laboratories Inc., Burlingame, CA, USA), and visualized using a Fluorescence Microscope BZ-9000 (Keyence Corp., Osaka, Japan). Images were captured digitally in real time and processed using BZ-II imaging software (Keyence Corp.).

Quantitative real-time reverse transcription polymerase chain reaction (RT-PCR)

Total RNA was isolated from cells with TRIzol reagent (Invitrogen). Samples were reverse transcribed with q-Srcipt cDNA Supermix reagents (Quanta BioSciences, Gaithersburg, MD, USA) and amplified for 30 min at 42°C. For real-time RT-PCR, the PCR products were detected using FAST® SYBR Green Master Mix (Applied Biosystems, Foster City, CA, USA) using the following primer sequences: *Gapdh* forward; 5′-GACGGCCGCATCTTCTTGA-3′ and reverse; 5′-CACACCGACCTTCACCATTTT-3′, and *Rankl* forward; 5′-GGCCAC AGCGCTTCTCA-3′ and reverse; 5′-CCTCGCTGGGCCACATC-3′. Thermal cycling and fluorescence detection were performed using a StepOne™ Real-Time System (Applied Biosystems). Real-time RT-PCR efficiency for each primer set was calculated according to the method of Rasmussen *et al.*[27] The fold increase in copy numbers of mRNA was calculated as the relative ratio of the *Rankl* gene to *Gapdh*, following the model of Pfaffl.[28]

Western blot analysis

Following incubation, total protein was extracted using Cell Lysis Buffer (Cell Signaling Technology) containing a protease inhibitor cocktail (Thermo Fisher Scientific, Waltham, MA, USA) and protein contents were measured using a DC protein assay kit (Bio-Rad, Hercules, CA, USA). Twenty micrograms of total protein per sample was loaded and separated on a Mini-PROTEAN TGX 4–15% gradient SDS-PAGE gel (Bio-Rad), then transferred onto polyvinylidene difluoride membranes (Millipore Corp., Bedford, MA, USA). Nonspecific binding sites were blocked by immersing the membranes in 5% skim milk in PBS for 1 h at room temperature. Membranes were subjected to incubation overnight with diluted primary antibodies at 4°C, followed by horseradish peroxidase (HRP) conjugated secondary antibodies for 1 h at room temperature. After washing the membranes, chemiluminescence was produced using ECL reagent (Amersham Pharmacia Biotech, Uppsala, Sweden) and detected digitally with a GelDoc™ XR Plus System (Bio-Rad). Goat anti-RANKL and mouse anti-β-actin were used as the primary antibodies, while HRP-conjugated anti-goat IgG (Santa

Cruz Biotechnology) and anti-mouse IgG (GE Healthcare, Little Chalfont, UK) were used as secondary antibodies.

RhoA activity

The amount of active RhoA was measured by using a pull-down assay with Rho Assay Reagent (Millipore Corp.), according to the manufacturer's instructions. Briefly, treated cells were washed twice in ice-cold PBS and lysed in lysis buffer (125 mM HEPES pH 7.5, 750 mM NaCl, 5% Igepal CA-630, 50 mM $MgCl_2$, 5 mM EDTA, 10 % glycerol), then the lysates were clarified by centrifugation at 14,000 × g for 5 min. Thereafter, the supernatant was incubated with Rhotekin-Rho binding domain beads for 45 min with gentle agitation at 4°C, after which the beads were washed 3 times with lysis buffer, followed by re-suspension in 40 μl of Laemmli reducing sample buffer. Precipitated GTP-bound and total RhoA proteins were then analyzed using western blotting analysis with an anti-RhoA monoclonal antibody.

Osteoclast formation in co-culture system

Osteoclasts were detected by staining with tartrate-resistant acid phosphatase (TRAP) using an Acid Phosphatase Leukocyte Kit (Sigma–Aldrich). In brief, ST2 cells (5×10^2 cells/well) were plated in a 96-well plate with αMEM containing 10% FBS and 10^{-7} M $1,25(OH)_2D_3$ (Sigma–Aldrich) in the presence or absence of HMW-HA (50 μg/ml). The next day, mouse monocyte RAW 264.7 cells (Riken Cell Bank, Ibaraki, Japan, 1×10^3 cells/well) were overlaid for the co-culture system. After co-culturing for 7 days, adherent cells were fixed and stained for TRAP activity, with TRAP-positive multinucleated cells containing three or more nuclei counted under a microscope as osteoclast-like cells.

Statistics analysis

All statistics analyses were carried out using JMP® software, version 10.0.2 (SAS Institute Inc., Cary, NC, USA). Each of the data groups was tested by using Shapiro–Wilk test and considered to follow a Gaussian distribution when the *P*-value was greater than 0.05. The Levene's test of homogeneity was used to determine the homogeneity of variance. All data were expressed as mean ± standard deviation and analyzed by one-way analysis if variance (ANOVA) and if significant, followed by the suitable post-test (Dunnett's or Tukey's post-test).

Results

HMW-HA down-regulates RANKL expression

We examined the effects of HMW-HA on RANKL expression in ST2 cells. The binding of HMW-HA (50 μg/ml) was monitored using an HABP probe and time-dependent HA binding could be visualized up to 3 h [Fig. 1(A)]. Primer sets for real-time RT-PCR amplification and quantification of mouse *Rankl* and *Gapdh* were designed, and

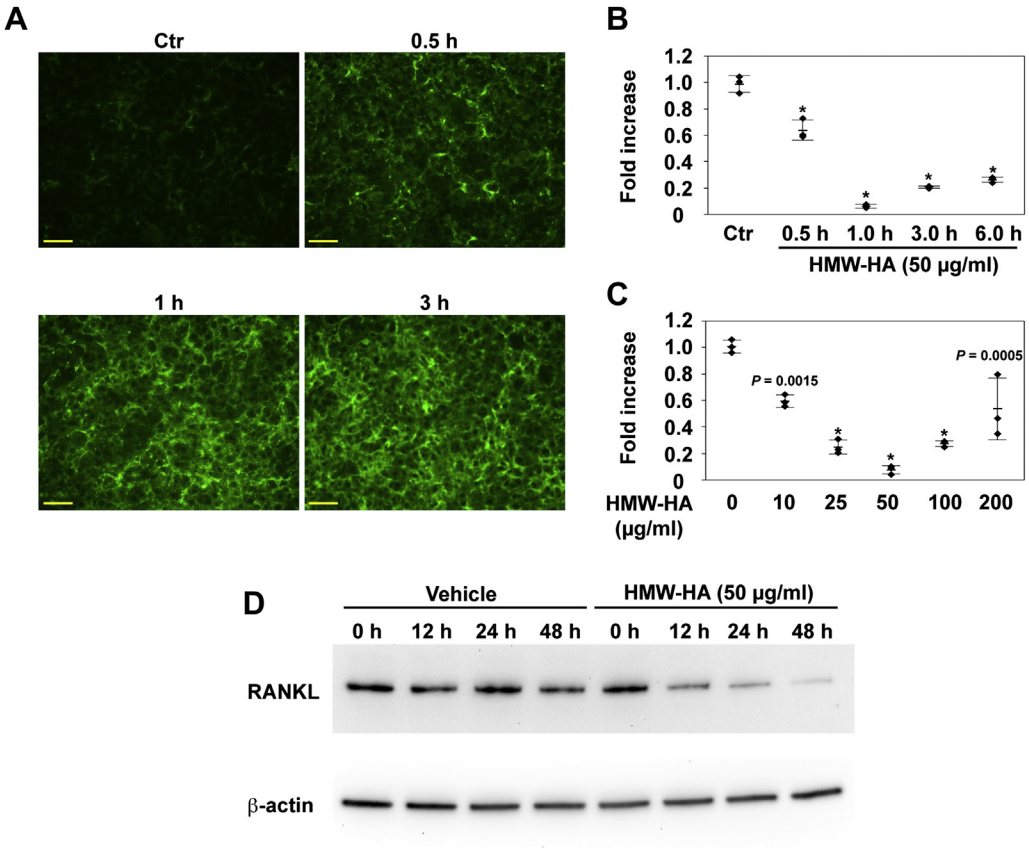

Fig. 1. Effect of HMW-HA on RANKL expression in ST2 cells. ST2 cells were incubated in the presence or absence of HMW-HA for varying times and in various concentrations. (A) Cells were incubated with a biotinylated HABP probe and HA accumulation was visualized using neutravidin-FITC. Bars indicate 10 μm. (B) Time course (ANOVA: $P < 0.0001$) and (C) concentration dependency (ANOVA: $P < 0.0001$) of *Rankl* mRNA stimulation by HMW-HA was determined by real-time RT-PCR. Data shows the fold changes in *Rankl* mRNA copy number values from independent samples of $n = 3$, and bars represent means with the standard deviation. Data were analyzed by Dunnett's test after one-way ANOVA. The asterisk indicates $P < 0.0001$ in comparison to control without any treatment. (D) Whole cell lysates were subjected to SDS-PAGE and western blotting analyses, with the blots probed for RANKL. Equivalent protein aliquots of cell lysates were also analyzed for β-actin.

the amplification efficiency of each set was determined, allowing for comparison of mRNA copy numbers between treated and control cultures, which were normalized to *Gapdh*. After 0.5 h of incubation with HMW-HA, there was a 26.4% decrease in *Rankl* mRNA copy number as compared to the untreated control cells [Fig. 1(B)]. This effect of HMW-HA was time-dependent, with maximum inhibition observed at the 1-h time point (96.3% inhibition). A concentration-dependent inhibition of *Rankl* by HMW-HA was also shown [Fig. 1(C)], which reached a maximum at a concentration of 50 μg/ml following 1 h of treatment (93% inhibition). As shown in [Fig. 1(D)], ST2 cell lysates from the control cultures expressed immunoreactive RANKL protein, while treatment with HMW-HA reduced RANKL protein expression in the ST2 cells for up to 48 h.

4-MU up-regulates RANKL expression

Next, we investigated whether the receptor-HA pathway has an influence on the expression of RANKL in ST2 cells using 4-MU. It has been reported that 4-MU inhibits HA synthesis and pericellular HA matrix formation in cultured cells.[29,30] We found a time-dependent decrease in accumulation of endogenous HA for up to 6 h following treatment with 4-MU (0.5 mM) [Fig. 2(A)]. Real-time RT-PCR also revealed an 8.1-fold increase in *Rankl* mRNA copy number as compared to the untreated control cells after 3 h of incubation with HMW-HA [Fig. 2(B)]. This effect of 4-MU was time-dependent, with maximum enhancement observed at the 6-h time point (12.1-fold increase). In addition, 4-MU induced a concentration-dependent stimulation of *Rankl* [Fig. 1(C)], with maximum stimulation observed at a concentration of 0.5 mM at 6 h after treatment (9.5-fold increase). Treatment with 4-MU also up-regulated RANKL protein expression in ST2 cells for up to 48 h [Fig. 2(D)].

Changes in matrix interactions by HA affect RANKL accumulation

ST2 cells at all examined culture times exhibited a background level of RANKL that was primarily localized on the cell surface [Fig. 3(A)]. No immunofluorescent staining was seen with the secondary antibody alone [Fig. 3(B)]. After 24 h of treatment with HMW-HA, RANKL protein accumulation was diminished [Fig. 3(C)]. On the other hand, after 24 h of treatment with 4-MU, RANKL levels were substantially enhanced [Fig. 3(D)].

CD44 function-blocking monoclonal antibody reverses reduction of RANKL expression induced by HMW-HA

To further examine the role of CD44 as an HA receptor in down-regulation of RANKL, ST2 cells were pre-treated with the CD44 function-blocking monoclonal antibody for 2 h prior to stimulation with HMW-HA. Treatment with the monoclonal antibody inhibited exogenous HMW-HA binding after 1 h of incubation [Fig. 4(A)]. Also, pretreatment with the monoclonal antibody effectively recovered the down-regulation of *Rankl* mRNA induced by 1 h of treatment with HMW-HA [Fig. 4(B)]. Western blotting analysis

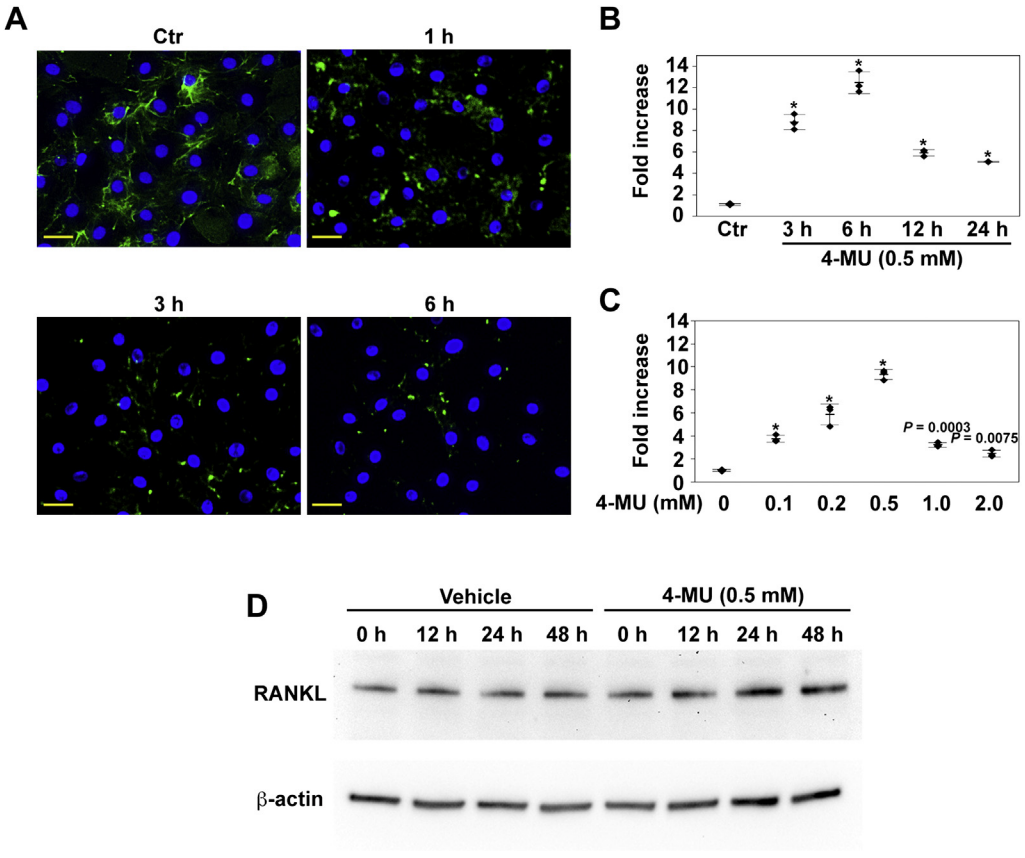

Fig. 2. Effect of 4-MU on RANKL expression in ST2 cells. ST2 cells were incubated in the presence or absence of 4-MU for varying times and in various concentrations. (A) Cells were incubated with a biotinylated HABP probe and HA accumulation was visualized using neutravidin-FITC. Coverslips were mounted in medium containing DAPI. Bars indicate 10 μm. (B) Time course (ANOVA: $P < 0.0001$) and (C) concentration dependency (ANOVA: $P < 0.0001$) of *Rankl* mRNA stimulation by 4-MU was determined by real-time RT-PCR. Data shows the fold changes in *Rankl* mRNA copy number values from independent samples of $n = 3$, and bars represent means with the standard deviation. Data were analyzed by Dunnett's test after one-way ANOVA. The asterisk indicates $P < 0.0001$ in comparison to control without any treatment. (D) Whole cell lysates were subjected to SDS-PAGE and western blotting analyses, with the blots probed for RANKL. Equivalent protein aliquots of cell lysates were also analyzed for β-actin.

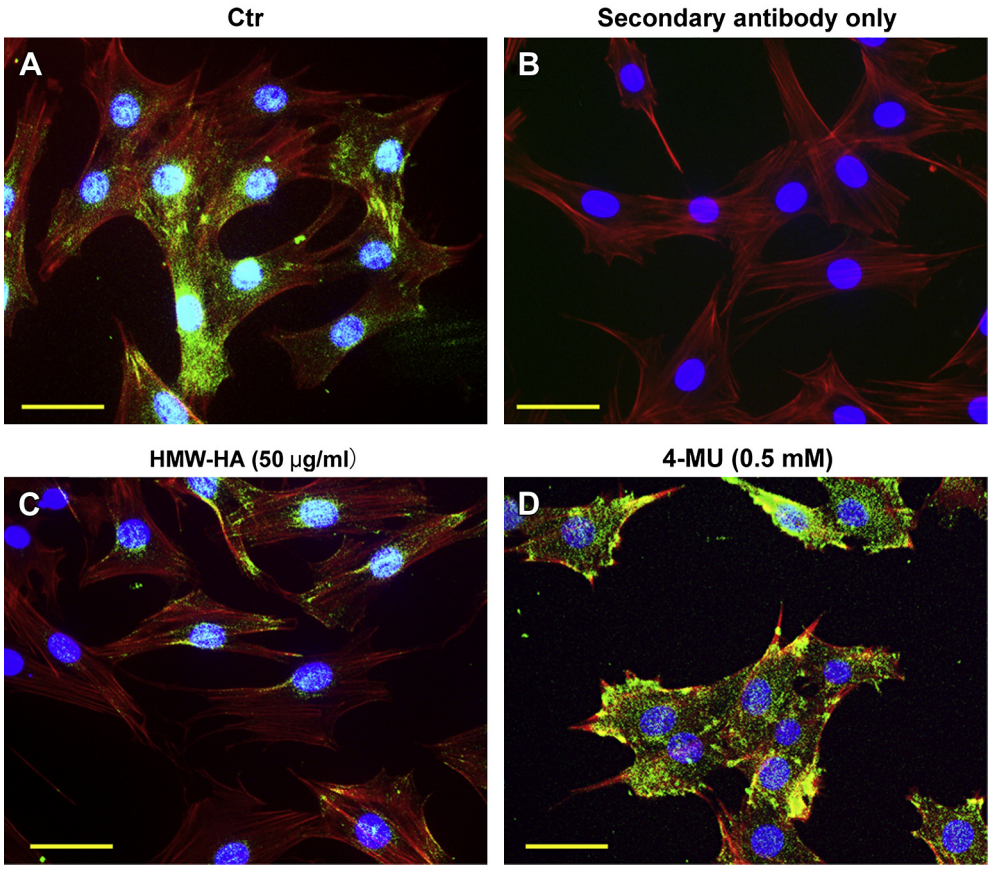

Fig. 3. Effect of HA accumulation on RANKL expression in ST2 cells. ST2 cells were grown on chamber slides, then incubated in the (A) absence or presence (C) of 50 μg/ml of HMW-HA, (D) or 0.5 mM of 4-MU for 24 h. Following treatment, the cells were fixed and immunostained using a polyclonal antibody to detect RANKL and rhodamine isothiocyanate-phalloidin. Coverslips were mounted in medium containing DAPI. (B) Control cells incubated with the secondary antibody alone. Shown are digital overlay images of red, green, and blue fluorescence channels. Bars indicate 20 μm.

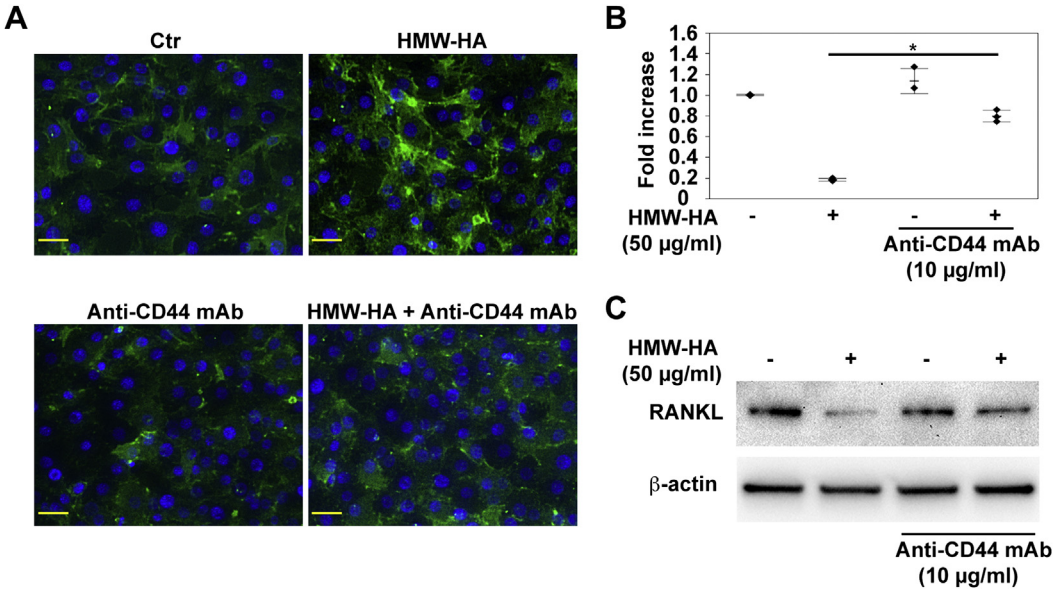

Fig. 4. Effects of CD44 function-blocking antibody on RANKL expression regulated by HMW-HA. ST2 cells were pretreated with or without 10 μg/ml of the CD44 function-blocking monoclonal antibody (CD44 mAb) for 2 h, then incubated in the presence or absence of HMW-HA (50 μg/ml) for the indicated time periods. (A) Cells were incubated with a biotinylated HABP probe and HA accumulation was visualized using neutravidin-FITC. Coverslips were mounted in medium containing DAPI. Bars indicate 10 μm. (B) Total RNA was isolated, and reverse transcribed into cDNA, then PCR amplification was performed using primers specific for *Rankl* and *Gapdh*. Data shows the fold changes in *Rankl* mRNA copy number values from independent samples of $n = 3$, and bars represent means with the standard deviation. Data were analyzed by Tukey's post-test after one-way ANOVA ($P < 0.0001$). The asterisk indicates $P < 0.0001$ in comparison to treatment with HMW-HA. (C) Whole cell lysates were subjected to SDS-PAGE and western blotting analyses, with the blots probed for RANKL. Equivalent protein aliquots of cell lysates were also analyzed for β-actin.

revealed that the monoclonal antibody also recovered the down-regulation of RANKL protein expression mediated after 24 h of incubation with HMW-HA [Fig. 4(C)].

Interaction between HMW-HA and CD44 induces sequential activation of RhoA protein

Recent findings indicate that the Rho kinase pathway has important roles in bone metabolism.[31–33] Therefore, we next examined whether HMW-HA induces RhoA activation in ST2 cells. RhoA activity was assessed by detecting GTP-loaded forms of the protein using a pull-down assay. As shown in [Fig. 5(A)], HMW-HA transiently activated RhoA in ST2 cells from 15 to 60 min, while RhoA activity returned to the basal level at 120 min of HMW-HA stimulation. Pre-treatment with the CD44 function-blocking monoclonal antibody inhibited the activation of RhoA protein mediated by HMW-HA stimulation for 30 min [Fig. 5(B)].

Rho/ROCK inhibitors attenuate down-regulation of RANKL expression mediated by HMW-HA

To further examine the role of RhoA activation in HMW-HA-mediated down-regulation of RANKL, ST2 cells were pre-treated with a Rho inhibitor (simvastatin) or selective Rho-associated protein kinase (ROCK) inhibitor (Y27632) for 24 h prior to stimulation with HMW-HA. Pretreatment with these inhibitors effectively blocked the down-regulation of *RANKL* mRNA [Fig. 6(A)] and RANKL protein [Fig. 6(B)] by HMW-HA.

HMW-HA inhibits osteoclast formation supported by ST2 cells

To determine whether HMW-HA has an influence ton ST2 cell-supported osteoclast formation, cells were treated with $1,25(OH)_2D_3$, which markedly stimulated *Rankl* mRNA expression in the ST2 cells for up to 24 h, while the addition of HMW-HA decreased the response of the cells to $1,25(OH)_2D_3$ [Fig. 7(A)]. As shown in [Fig. 7(B)], the level of RANKL protein expression was increased in ST2 cells at 48 h after stimulation with $1,25(OH)_2D_3$ and that stimulation was down-regulated by addition of HMW-HA. Western blotting analysis also revealed that pre-treatment with the Rho/ROCK inhibitors attenuated the down-regulation of RANKL protein in $1,25(OH)_2D_3$-stimulated ST2 cells mediated by HMW-HA.

To further clarify the role of the HMW-HA in osteoclastogenesis, we cocultured mouse monocytes (RAW 264.7 cells), as osteoclast precursors with ST2 cells pre-stimulated with $1,25(OH)_2D_3$. As shown in [Fig. 7(C) and (D)], culturing with HMW-HA down-regulated the differentiation of RAW 264.7 cells into osteoclast-like cells induced by $1,25(OH)_2D_3$-stimulated ST2 cells.

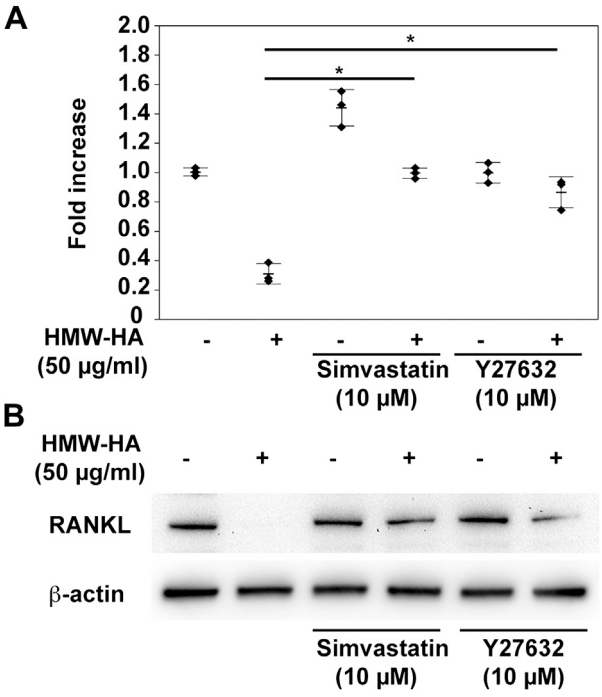

Fig. 6. Effects of RhoA/ROK inhibitors on RANKL expression regulated by HMW-HA. ST2 cells were pretreated with simvastatin (10 μM) or Y27632 (10 μM) for 24 h, then incubated in the presence or absence of HMW-HA (50 μg/ml) for the indicated time periods. (A) Total RNA was isolated, and reverse transcribed into cDNA, then PCR amplification was performed using primers specific for *Rankl* and *Gapdh*. Data shows the fold changes in *Rankl* mRNA copy number values from independent samples of $n = 3$, and bars represent means with the standard deviation. Data were analyzed by Tukey's post-test after one-way ANOVA ($P < 0.0001$). The asterisk indicate $P < 0.0001$ in comparison to treatment with HMW-HA. (B) Whole cell lysates were subjected to SDS-PAGE and western blotting analyses, with the blots probed for RANKL. Equivalent protein aliquots of cell lysates were also analyzed for β-actin.

Discussion

Bone resorption has been reported to be increased in women with progressive knee OA as compared to those with non-progressive disease[34]. Furthermore, peripheral blood mononuclear cells from patients with OA have been shown to exhibit enhanced capacity to generate osteoclasts and higher levels of bone

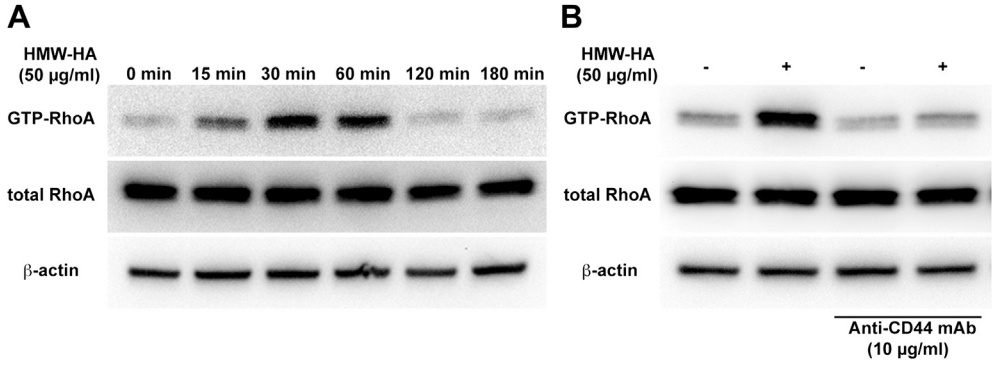

Fig. 5. Effects of HMW-HA on RhoA activation in ST2 cells. (A) ST2 cells were incubated in the presence or absence of 50 μg/ml of HMW-HA for the indicated time periods. (B) ST2 cells were pretreated with or without 10 μg/ml CD44 mAb for 2 h, then incubated with HMW-HA (50 μg/ml) for 30 min. Whole cell lysates were subjected to SDS-PAGE and western blot analyses, with the blots probed for anti-RhoA (total RhoA). Equivalent protein aliquots of cell lysates were also analyzed for β-actin. GTP-RhoA was isolated utilizing GST-Rhotekin RBD, followed by SDS-PAGE and western blot analyses with the anti-RhoA antibody.

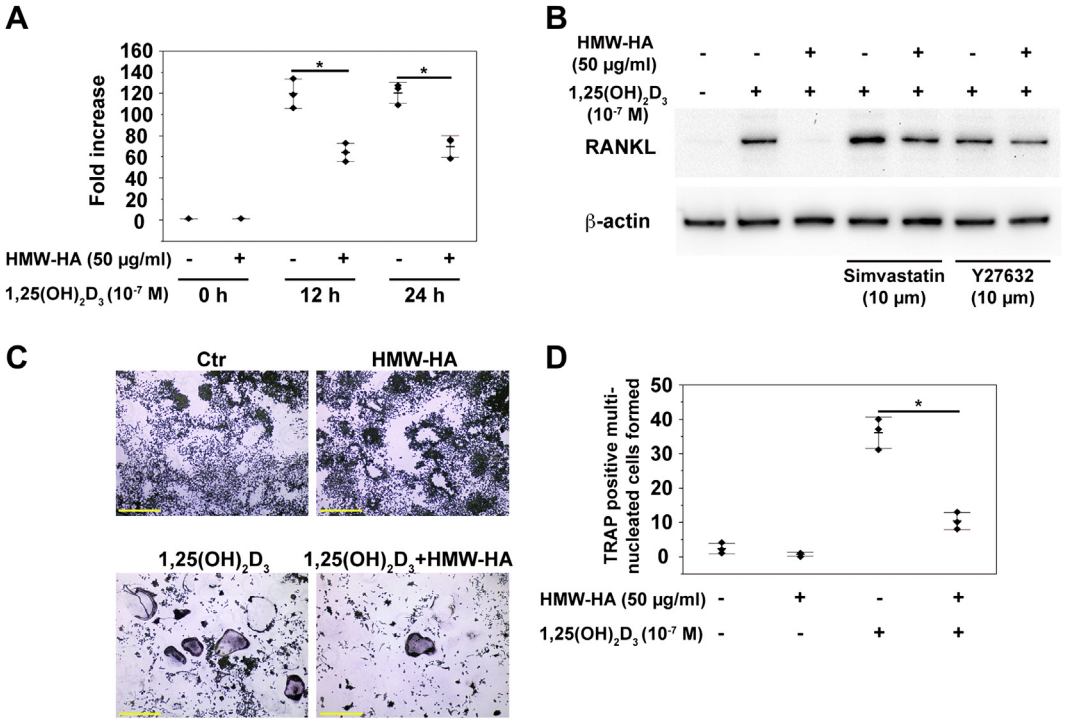

Fig. 7. Effects of HMW-HA on osteoclast formation supported by ST2 cells. (A) ST2 cells were stimulated with 1,25$(OH)_2D_3$ (10^{-7} M) in the presence or absence of HMW-HA (50 μg/ml) for the indicated times. Total RNA was isolated and reverse transcribed into cDNA, then PCR amplification was performed using primers specific for *Rankl* and *Gapdh*. Data shows the fold changes in *Rankl* mRNA copy number values from independent samples of $n = 3$, and bars represent means with the standard deviation. Data were analyzed by Tukey's post-test after one-way ANOVA ($P < 0.0001$). The asterisk indicates $P < 0.0001$ in comparison to treatment with 1,25$(OH)_2D_3$. (B) ST2 cells were pretreated with simvastatin (10 μM) or Y27632 (10 μM) for 24 h, then incubated with 1,25$(OH)_2D_3$ (10^{-7} M) in the presence or absence of HMW-HA (50 μg/ml) for 48 h. Whole cell lysates were subjected to SDS-PAGE and western blotting analyses, with the blots probed for RANKL. Equivalent protein aliquots of cell lysates were also analyzed for β-actin. (C) ST2 cells were pre-treated with 1,25$(OH)_2D_3$ (10^{-7} M) in the presence or absence of HMW-HA (50 μg/ml) for 24 h, then co-cultured with RAW 264.7 cells for 6 days and stained for TRAP activity. Bars indicate 500 μm. (D) The number of osteoclast-like cells was counted after the staining for TRAP activity. Data shows the number of osteoclast-like cells from independent samples of $n = 3$, and bars represent means with the standard deviation. Data were analyzed by Tukey's post-test after one-way ANOVA ($P < 0.0001$). The asterisk indicates $P < 0.0001$ in comparison to treatment with 1,25$(OH)_2D_3$.

resorption *in vitro*[35], while inhibition of osteoclastic activity by bisphosphonate was found to prevent bone and cartilage resorption in a rat degenerative joint disease model[36]. Therefore, there is great interest in identifying the effects of HMW-HA on osteoclastogenesis as a target for developing therapeutic agents to prevent joint destruction in OA.

In the present study, we used a homogeneous clonal population of mouse bone marrow stromal ST2 cells to elucidate the effects of HMW-HA on induction of osteoclast differentiation. This cell line is known to highly express RANKL in the presence of 1,25$(OH)_2D_3$ and RANKL-expressing cells support the differentiation of splenic cells into osteoclasts[37]. The main advantage of the present system is that it does not contain any pre-osteoclast cells, which may also be targets of HMW-HA activities.

As shown in Figs. 1 and 3, RANKL mRNA and protein were decreased by addition of HMW-HA, indicating that it has protective effects against osteoclastogenesis. Chang *et al.* reported that HMW-HA (1,300 kDa) decreased osteoclast formation by bone marrow-derived macrophages and human peripheral blood monocytic cells, but not by RAW 264.7 cells[25]. In the study, they discussed that the difference in effects of HMM-HA between RAW 264.7 cells and primary osteoclast precursors may be ascribed to the independence of RAW 264.7 cells on macrophage colony stimulating factor (M-CSF) for proliferation and osteoclastic differentiation. Furthermore, our results would suggest that suppression of osteoclastogenesis by HMW-HA is also dependent on down-regulation of RANKL expression in osteoblasts/stromal cells. In contrast to those findings, Cao *et al.* reported that HMW-HA stimulated RANKL expression in bone marrow stromal cells[38]. We have no ready explanation for these contrasting results, though it is possible that they reflect differences in the cell species tested or variations in culture conditions, including the presence or absence of serum.

The modified coumarin, 4-MU has been reported to specifically inhibit HA synthesis and pericellular HA matrix formation in cultured mammalian cells[29,30]. Several studies have reported the various biological effects of 4-MU on inflammatory response in arthritis[39], tumourigenicity[40], and nerve injury[41]. As shown in Figs. 2 and 3, we found that 4-MU up-regulated RANKL expression, and our observations suggest that inhibition of HA synthesis and loss of cell–matrix interaction enhance osteoclast differentiation and bone resorption. In addition, the effect of 4-MU on proliferation of ST2 cells was examined using a WST-1 assay, though no effect on cell growth up to 48 h was seen.

Another important finding of our study is that the HA receptor CD44 is required for down-regulation of RANKL mediated by HMW-HA. CD44 is one of the major HA binding proteins and expressed in several types of cells, including osteoblasts[42], while binding of HA to CD44 is known to be involved in onset of a variety of biological activities. The monoclonal rat anti-CD44 antibody recognizes a determinant of the HA binding region common to CD44 and its principal variant isoforms[43] and that antibody is routinely used in HA-related blocking experiments. As shown in [Fig. 4(A)], pre-treatment with that CD44 function-blocking monoclonal antibody resulted in significantly reduced accumulation of exogenous HMW-HA in ST2 cells. We also found that this antibody remarkably inhibited the effect of HMW-HA on down-regulation of RANKL in ST2 cells [Fig. 4(B) and (C)]. On the basis of these findings, we speculate that expression of CD44 in

ST2 cells, which have the same lineage as osteoblasts, leads to regulation of osteoclast formation and activation mediated by HMW-HA.

Rho GTPases (RhoA, Rac1, Cdc42) are members of the Rho subclass of the Ras superfamily[44], and have a cycle between active GTP-bound states and inactivate GDP-bound states in response to external stimuli. In their active form, they regulate key signaling pathways and control a variety of cellular activities, including gene transcription, cytoskeleton reorganization, cell growth, migration, and oncogenesis[45]. Previous studies have also found that HA-CD44 binding induces RhoA signaling in head and neck tumor cells[46]. In the present study, addition of HMW-HA led to a significant increase in the level of active GTP-bound RhoA [Fig. 5(A)], while pre-treatment with the CD44 function-blocking monoclonal antibody remarkably inhibited HMW-HA-induced RhoA activation in ST2 cells [Fig. 5(B)]. These results demonstrated that HA-CD44 interaction also induces RhoA signaling in osteoblasts/stromal cells.

Recent findings indicate that the RhoA signaling pathway has important roles in bone remodeling. For example, in osteoblast survival[31], the integrity of the actin cytoskeleton[32], as well as migration and differentiation[33] are regulated by RhoA signaling. Simvastatin has been reported to reduce the synthesis of mevalonate by inhibiting hydroxymethylglutaryl (HMG)-CoA reductase, finally leading to blockade of Rho GTPases by the effector proteins ROCK[47]. On the other hand, Y-27632, a pyridine derivative, was discovered to particularly disrupt ROCK signaling[48] and has been widely investigated in various studies. We found that blockage the RhoA/ROCK pathway by either simvastatin or Y-27632 prevented a decrease in RANKL expression caused by exposure to HMW-HA [Fig. 6]. These findings are consistent with a previous study, in which the expression of constitutively active RhoA in osteoblastic cells was shown to impair their ability to induce osteoclastogenesis via suppression of RANKL mRNA in response to parathyroid hormone or calcitol.[49]

As a catabolic effect on bone, $1\alpha,25(OH)_2D_3$ promotes osteoclastogenesis by up-regulating the expression of RANKL. In the present study, administration of HMW-HA decreased RANKL expression induced by $1\alpha,25(OH)_2D_3$ [Fig. 7(A)], while simvastatin and Y-27632 recovered that decreased expression in cells treated with HMW-HA [Fig. 7(B)]. HMW-HA also prevented osteoclast differentiation of co-cultured precursors supported by stromal cells expressing RANKL [Fig. 7(C) and (D)]. These results suggest that activation of RhoA/Rho kinase signaling by HMW-HA inhibits RANKL in bone marrow stromal cells, thereby inhibiting osteoclastogenesis. Furthermore, $1\alpha,25(OH)_2D_3$ was reported to suppress the gene expression of osteoprotegerin (OPG), which acts as a decoy receptor for RANKL and prevents RANK–RANKL interaction, and thus osteoclastogenesis[50]. In our study, HMW-HA recovered up-regulation of RANKL expression, while the down-regulation of OPG was mediated by $1\alpha,25(OH)_2D_3$ (data not shown). Bone resorption is a multistep process initiated by the proliferation of immature osteoclast precursors, which is followed by the commitment of those cells to the osteoclast phenotype and degradation of the organic and inorganic phases of bone by mature resorptive cells. We previously reported that TRAP positive multinucleated cells differentiated from RAW 264.7 cells by RANKL are capable of bone resorption using calcium phosphate substrate coated slides[26]. From those results, the molecular mechanism for the effect of HMW-HA on OPG expression and on osteoclast function are currently under investigation in our laboratory.

HA is known to be associated with several cell surface molecules, such as CD44, receptor for hyaluronan-mediated motility (RHAMM), toll-like receptor-4 (TLR4), and intercellular adhesion molecule (ICAM-1). It has also been reported that RHAMM, TLR4, and ICAM-1 are expressed in osteoblast stromal lineage cells. Further study is needed to examine the correlations between HMW-HA and other receptors regarding inhibition of osteoclast formation, as well as signal transduction during osteoclastogenesis.

In conclusion, the present findings showed that HMW-HA inhibits the transcription of RANKL in stromal cells by activating the RhoA/Rho kinase pathways. CD44-mediated signaling supports this activation and is likely critical for certain cell types, such as stromal cells. Furthermore, our results suggest that stromal cells have a capacity to sense changes in cell surface HA-CD44 interactions, resulting in regulation of bone metabolism. Whether analogous effect of HMW-HA on osteoclast occurs in human cells or *in vivo* animal model remains to be determined. Nonetheless, we consider that these results provide a basis to understand why HMW-HA is effective when used as treatment for OA.

Author contributions

All of the authors were involved in drafting the article or critically revising it for important intellectual content, and all approved the final version to be published. Dr. T. Nishihara had full access to all of the data in the study, and takes responsibility for its integrity and the accuracy of the data analysis.

Study conception and design: Ariyoshi W, Okinaga T, Nishihara T.

Acquisition of data: Ariyoshi W, Knudson C.B, Knudson W, Nishihara T.

Analysis and interpretation of data: Ariyoshi W, Okinaga T, Nishihara T.

Conflicts of interest

The authors have no conflicts of interest to disclose.

Acknowledgments

This work was supported by a Grant-in-Aid for Scientific Research from Japan Society for the Promotion of Science.

References

1. Lee JY, Spicer AP. Hyaluronan: a multifunctional, megaDalton, stealth molecule. Curr Opin Cell Biol 2000;12:581–6.
2. Noble PW. Hyaluronan and its catabolic products in tissue injury and repair. Matrix Biol 2002;21:25–9.
3. Goldberg VM, Buckwalter JA. Hyaluronans in the treatment of osteoarthritis of the knee: evidence for disease-modifying activity. Osteoarthritis Cartilage 2005;13:216–24.
4. Amiel D, Toyoguchi T, Kobayashi K, Bowden K, Amiel ME, Healey RM. Long-term effect of sodium hyaluronate (Hyalgan) on osteoarthritis progression in a rabbit model. Osteoarthritis Cartilage 2003;11:636–43.
5. Abatangelo G, Botti P, Del Bue M, Gei G, Samson JC, Cortivo R, *et al.* Intraarticular sodium hyaluronate injections in the Pond-Nuki experimental model of osteoarthritis in dogs. I. Biochemical results. Clin Orthop Relat Res 1989;241:278–85.
6. Altman RD, Moskowitz R. Intraarticular sodium hyaluronate (Hyalgan) in the treatment of patients with osteoarthritis of the knee: a randomized clinical trial. Hyalgan Study Group. J Rheumatol 1998;25:2203–12.
7. Kolarz G, Kotz R, Hochmayer I. Long-term benefits and repeated treatment cycles of intra-articular sodium hyaluronate (Hyalgan) in patients with osteoarthritis of the knee. Semin Arthritis Rheum 2003;32:310–9.
8. Knudson W, Aguiar DJ, Hua Q, Knudson CB. CD44-anchored hyaluronan-rich pericellular matrices: an ultrastructural and biochemical analysis. Exp Cell Res 1996;228:216–28.

9. Assimakopoulos D, Kolettas E, Patrikakos G, Evangelou A. Histol Histopathol 2002;17:1269–81.
10. Bourguignon LY, Singleton PA, Zhu H, Diedrich F. Hyaluronan-mediated CD44 interaction with RhoGEF and Rho kinase promotes Grb2-associated binder-1 phosphorylation and phosphatidylinositol 3-kinase signaling leading to cytokine (macrophage-colony stimulating factor) production and breast tumor progression. J Biol Chem 2003;278:29420–34.
11. Bourguignon LY, Zhu H, Shao L, Chen YW. CD44 interaction with tiam1 promotes Rac1 signaling and hyaluronic acid-mediated breast tumor cell migration. J Biol Chem 2000;275:1829–38.
12. Bourguignon LY, Zhu H, Zhou B, Diedrich F, Singleton PA, Hung MC. Hyaluronan promotes CD44v3-Vav2 interaction with Grb2-p185(HER2) and induces Rac1 and Ras signaling during ovarian tumor cell migration and growth. J Biol Chem 2001;276:48679–92.
13. Bourguignon LY, Zhu H, Shao L, Chen YW. CD44 interaction with c-Src kinase promotes cortactin-mediated cytoskeleton function and hyaluronic acid-dependent ovarian tumor cell migration. J Biol Chem 2001;276:7327–36.
14. Bourguignon LY, Singleton PA, Zhu H, Zhou B. Hyaluronan promotes signaling interaction between CD44 and the transforming growth factor beta receptor I in metastatic breast tumor cells. J Biol Chem 2002;277:39703–12.
15. Kohda D, Morton CJ, Parkar AA, Hatanaka H, Inagaki FM, Campbell ID, *et al*. Solution structure of the link module: a hyaluronan-binding domain involved in extracellular matrix stability and cell migration. Cell 1996;86:767–75.
16. Suda T, Takahashi N, Martin TJ. Modulation of osteoclast differentiation. Endocr 1992;13:66–80.
17. Suda T, Takahashi N, Udagawa N, Jimi E, Gillespie MT, Martin TJ. Modulation of osteoclast differentiation and function by the new members of the tumor necrosis factor receptor and ligand families. Endocr Rev 1999;20:345–57.
18. Darnay BG, Haridas V, Ni J, Moore PA, Aggarwal BB. Characterization of the intracellular domain of receptor activator of NF-κB (RANK): interaction with tumor necrosis factor receptor-associated factors and activation of NF-κB and c-Jun N-terminal kinase. J Biol Chem 1998;273:20551–5.
19. Fioravanti A, Cantarini L, Chellini F, Manca D, Paccagnini E, Marcolongo R, *et al*. Effect of hyaluronic acid (MW 500-730 kDa) on proteoglycan and nitric oxide production in human osteoarthritic chondrocyte cultures exposed to hydrostatic pressure. Osteoarthritis Cartilage 2005;13:688–96.
20. Tanaka M, Masuko-Hongo K, Kato T, Nishioka K, Nakamura H. Suppressive effects of hyaluronan on MMP-1 and RANTES production from chondrocytes. Rheumatol Int 2006;26:185–90.
21. Wang CT, Lin YT, Chiang BL, Lin YH, Hou SM. High molecular weight hyaluronic acid down-regulates the gene expression of osteoarthritis-associated cytokines and enzymes in fibroblast-like synoviocytes from patients with early osteoarthritis. Osteoarthritis Cartilage 2006;14:1237–47.
22. Cake MA, Smith MM, Young AA, Smith SM, Ghosh P, Read RA. Synovial pathology in an ovine model of osteoarthritis: effect of intraarticular hyaluronan (Hyalgan). Clin Exp Rheumatol 2008;26:561–7.
23. Lajeunesse D, Delalandre A, Martel-Pelletier J, Pelletier JP. Hyaluronic acid reverses the abnormal synthetic activity of human osteoarthritic subchondral bone osteoblasts. Bone 2003;33:703–10.
24. Pivetta E, Scapolan M, Wassermann B, Steffan A, Colombatti A, Spessotto P. Blood-derived human osteoclast resorption activity is impaired by Hyaluronan-CD44 engagement via a p38-dependent mechanism. J Cell Phyiol 2011;226:763–9.
25. Chang EJ, Kim HJ, Ha J, Kim HJ, Ryu J, Park KH, *et al*. Hyaluronan inhibits osteoclast differentiation via toll-like receptor 4. J Cell Sci 2007;120:166–76.
26. Ariyoshi W, Takahashi T, Kanno T, Ichimiya H, Takano H, Koseki T, *et al*. Mechanisms involved in enhancement of osteoclast formation and function by low molecular weight hyaluronic acid. J Biol Chem 2005;280:18967–72.
27. Rasmussen TB, Uttenthal A, de Stricker K, Belak S, Storgaard T. Development of a novel quantitative real-time RT-PCR assay for the simultaneous detection of all serotypes of foot-and-mouth disease virus. Arch Virol 2003;148:2005–21.
28. Pfaffl MW. A new mathematical model for relative quantification in real-time RT-PCR. Nucleic Acids Res 2001;29:e45.
29. Kudo D, Kon A, Yoshihara S, Kakizaki I, Sasaki M, Endo M, *et al*. Effect of a hyaluronan synthase suppressor, 4-methylumbelliferone, on B16F-10 melanoma cell adhesion and locomotion. Biochem Biophys Res Commun 2004;321:783–7.
30. Nakazawa H, Yoshihara S, Kudo D, Morohashi H, Kakizaki I, Kon A, *et al*. 4-methylumbelliferone, a hyaluronan synthase suppressor, enhances the anticancer activity of gemcitabine in human pancreatic cancer cells. Cancer Chemother Pharmacol 2006;57:165–70.
31. Yoshida T, Clark MF, Stern PH. The small GTPase RhoA is crucial for MC3T3-E1 osteoblastic cell survival. J Cell Biochem 2009;106:896–902.
32. Kazmers NH, Ma SA, Yoshida T, Stern PH. Rho GTPase signaling and PTH 3-34, but not PTH 1-34, maintain the actin cytoskeleton and antagonize bisphosphonate effects in mouse osteoblastic MC3T3-E1 cells. Bone 2009;45:52–60.
33. Yang S, Tian YS, Lee YJ, Yu FH, Kim HM. Mechanisms by which the inhibition of specific intracellular signaling pathways increase osteoblast proliferation on apatite surfaces. Biomaterials 2011;32:2851–61.
34. Bettica P, Cline G, Hart DJ, Meyer J, Spector TD. Evidence for increased bone resorption in patients with progressive knee osteoarthritis: longitudinal results from the Chingford study. Arhthritis Rheum 2002;46:3178–84.
35. Durand M, Komarova SV, Bhargava A, Trebec-Reynolds DP, Li K, Fiorino C, *et al*. Monocytes from patients with osteoarthritis display increased osteoclastogenesis and bone resorption: the In vitro Osteoclast Differentiation in Arthritis study. Arthritis Rheum 2013;65:148–58.
36. Strassle BW, Mark L, Leventhal L, Piesla MJ, Jian Li X, Kennedy JD, *et al*. Inhibition of osteoclasts prevents cartilage loss and pain in a rat model of degenerative joint disease. Osteoarthritis Cartilage 2010;18:1319–28.
37. Udagawa N, Takahashi N, Akatsu T, Sasaki T, Yamaguchi A, Kodama H, *et al*. The bone marrow-derived stromal cell lines MC3T3-G2/PA6 and ST2 support osteoclast-like cell differentiation in cocultures with mouse spleen cells. Endocrinology 1989;125:1805–13.
38. Cao JJ, Singleton PA, Majumdar S, Boudignon B, Burghardt A, Kurimoto P, *et al*. Hyaluronan increases RANKL expression in bone marrow stromal cells through CD44. J Bone Miner Res 2005;21:30–40.
39. Yoshioka Y, Kozawa E, Urakawa H, Arai E, Futamura N, Zhuo L, *et al*. Suppression of hyaluronan synthesis alleviates inflammatory response in murine arthritis and in human rheumatoid synovial fibroblasts. Arthritis Rheum 2013;65:1160–70.
40. Arai E, Nishida Y, Wasa J, Urakawa H, Zhuo L, Kimata K, *et al*. Inhibition of hyaluronan retention by 4-methylumbelliferone

suppresses osteosarcoma cells in vitro and lung metastasis in vivo. Br J Cancer 2011;105:1839–49.
41. Yong N, Guoping C. Upregulation of matrix metalloproteinase-9 dependent on hyaluronan synthesis after sciatic nerve injury. Neurosci Lett 2008;444:259–63.
42. García-Martínez O, Reyes-Botella C, Aguilera-Castillo O, Vallecillo-Capilla MF, Ruiz C. Antigenic profile of osteoblasts present in human bone tissue sections. Biosci Rep 2006;26:39–43.
43. Bourguignon LY, Singleton PA, Diedrich F, Stern R, Gilad E. CD44 interaction with Na^{+}-H^{+} exchanger (NHE1) creates acidic microenvironments leading to hyaluronidase-2 and cathepsin B activation and breast tumor cell invasion. J Biol Chem 2004;279:26991–7007.
44. Hall A. Rho GTPases and the actin cytoskeleton. Science 1998;279:509–14.
45. Li X, Lim B. Rho GTPases and their role in cancer. Oncol Res 2003;13:323–31.
46. Bourguignon LY, Gilad E, Brightman A, Diedrich F, Singleton P. Hyaluronan-CD44 interaction with leukemia-associated RhoGEF and epidermal growth factor receptor promotes Rho/Ras co-activation, phospholipase Cε-Ca^{2+} signaling, and cytoskeleton modification in head and neck squamous cell carcinoma cells. J Biol Chem 2006;281:14026–40.
47. Fromigue O, Hay E, Modrowski D, Bouvet S, Jacquel A, Auberger P, *et al*. RhoA GTPase inactivation by statins induces osteosarcoma cell apoptosis by inhibiting p42/p44-MAPKs-Bcl-2 signaling independently of BMP-2 and cell differentiation. Cell Death Differ 2006;13:1845–56.
48. Uehata M, Ishizaki T, Satoh H, Ono T, Kawahara T, Morishita T, *et al*. Calcium sensitization of smooth muscle mediated by a Rho-associated protein kinase in hypertension. Nature 1997;389:990–4.
49. Wang J, Stern PH. Osteoclastogenic activity and RANKL expression are inhibited in osteoblastic cells expressing constitutively active Gα(12) or constitutively active RhoA. J Cell Biochem 2010;111:1531–6.
50. Kondo T, Kitazawa R, Maeda S, Kitazawa S. 1 alpha,25 dihydroxyvitamin D3 rapidly regulates the mouse osteoprotegerin gene through dual pathways. J Bone Miner Res 2004;19:1411–9.